The Journal of Experimental Biology 208, 3055-3063
Published by The Company of Biologists 2005
doi:10.1242/jeb.01755

Computer simulations of high-pass filtering in zebrafish larval muscle fibres

Steven D. Buckingham[1] and Declan W. Ali[2,*]

[1]*MRC Functional Genetics Unit, Department of Human Anatomy and Genetics, University of Oxford, South Parks Road, Oxford, OX1 3QX, UK* and [2]*University of Alberta, Department of Biological Sciences, Biological Sciences Building, Edmonton, Alberta, Canada, T6G 2E9*

*Author for correspondence (e-mail: declan.ali@ualberta.ca)

Accepted 15 June 2005

Summary

Larval somatic muscle of the zebrafish, *Danio rerio*, like that of some other organisms, responds to a sustained depolarization with one, and only one, action potential. Here, we report computer simulations, using the NEURON simulation programme, of sodium and potassium currents of somatic muscle of larval *Danio rerio* to investigate their possible contribution to once-only firing. Our computer model incorporated simulated sodium and potassium ion channels based on steady-state and kinetic parameters derived from a recent electrophysiological study. The model responded to sustained depolarizations with a single action potential at all levels of depolarization above threshold. By varying several parameters of the sodium and potassium currents systematically, the minimum changes necessary to produce repetitive firing were found to be a positive shift in the half-inactivation and a negative shift in the half-activation potentials for the sodium current, accompanied by a slowing of the rate of inactivation to half of the experimentally observed values. This suggests that once-only spiking can be attributed to the steady-state values of activation and inactivation of the sodium current, along with a slower rate of inactivation. Mapping of the resultant firing properties against steady-state and kinetic ion channel parameters revealed a high safety factor for once-only firing and showed that the time constant of inactivation of the sodium current was the key determinant of once-only or repetitive firing. The rapidly inactivating potassium current does not influence once-only firing or the maximum rate of firing in response to periodic excitation in these simulations. Although a contribution of other currents to produce once-only firing has not been excluded, this model suggests that the properties of the sodium current are sufficient to account for once-only firing.

Key words: ion channel, sodium, potassium, activation, inactivation, action potential.

Introduction

The zebrafish, *Danio rerio* Hamilton, is a particularly convenient model for experimental investigations into developing nervous and muscle systems. The advantages it offers include the invariant pattern of development of the somatic motor system (especially the trunk muscles that underlie swimming) and its ready accessibility to electrophysiological studies (Drapeau et al., 1999; Westerfield, 2000). Despite these advantages, the electrophysiological properties of the developing muscle in larvae of zebrafish have received surprisingly little attention (Buckingham and Ali, 2004; Buss and Drapeau, 2000). Zebrafish axial muscle is typical of teleost muscle in that it consists of both red and white fibre types (Greer-Walker and Pull, 1975; van Raamsdonk et al., 1979) with different behavioural roles (Buss and Drapeau, 2002).

A number of neurones in different organisms respond to a sustained depolarization with a short burst of spikes, sometimes with only one spike (Buss et al., 2003; Eliasof et al., 1987; Korn et al., 1990; Rothe et al., 1999; Torkkeli and French, 2002; Tsutsui et al., 2001). This represents a form of high-pass filtering, in which the input to the neurone is differentiated when in the increasing direction. The frequency of the phenomenon of once-only firing suggests that it is an important physiological adaptation. The ionic basis of this phenomenon, however, is often poorly understood. Furthermore, except in the case of sensory neurones showing rapid adaptation to sustained stimuli, the behavioural significance of high-pass filtering in many neurones is not clear. The white muscle fibres of the tail of developing *Danio rerio* support once-only, or single-spike, firing and are very convenient for patch-clamp studies (Buckingham and Ali, 2004; Buss and Drapeau, 2000; Drapeau et al., 1999), hence they offer a convenient model for the study of high-pass filtering in a well-defined behavioural context.

The phenomenon of once-only firing in fish muscle is thought to be an adaptation to the functional role of these muscles in swimming, which in larvae involves rhythmic contractions at rates up to 30 per second (Buss and Drapeau, 2000). Once-only

firing presumably ensures that the muscle can be activated at high frequencies without evoking tetanic contractions, which may compromise regular, rhythmic contractions. Currently, little is known of the ionic basis of once-only firing, although it occurs in a number of different neurones in both vertebrates and invertebrates. The spider VS-3 slit-sense organ, for example, contains two neurones, of which one exhibits once-only firing while the other fires tonically in response to a sustained stimulation (Seyfarth and French, 1994). In computer simulations of these neurones, altering two parameters – the slope of the steady-state inactivation curve and the time constant of inactivation of the sodium current – was sufficient to switch between these two patterns of firing (Torkkeli and French, 2002). Similarly, large cells in the corpus glomerulosum of adult filefish, *Stephanoplepis cirrhifer*, fire only once in response to a prolonged depolarization (Tsutsui et al., 2001). This phenomenon has been modelled by a computer simulation (Tsutsui and Oka, 2002), but the ionic events causing it were not explored. Immature retinal ganglion neurons (RGN) exhibit single-spike firing during postnatal days P1 to P11, thought to be a consequence of insufficient calcium-activated potassium current [$I_{K(Ca)}$], while retinal amacrine cells fire single spikes because of insufficient Na^+ conductance and a lack of removal of Na^+ inactivation (Eliasof et al., 1987).

In a recent paper in which we described the steady-state and kinetic properties of a sodium and potassium current present in the inner muscles of the zebrafish (Buckingham and Ali, 2004), we suggested that once-only firing may arise from the fact that the sodium current is rapidly inactivated and requires a rebound to more hyperpolarized voltages before sufficient channels are reactivated. Since at a resting potential of approximately –70 mV in the larvae (Buss and Drapeau, 2000) and approximately –80 mV in the adult (Westerfield et al., 1986) up to 70% of sodium current is inactivated (Buckingham and Ali, 2004), a second spike might only be possible after a hyperpolarization. We proposed that this hyperpolarization is provided by the rapidly inactivating potassium current. An alternative explanation (Adrian and Bryant, 1974; Bryant, 1962; Bretag, 1987) is that a voltage-gated chloride current provides a shunt, preventing a second spike during a prolonged depolarization. Since it is extremely difficult to manipulate the steady-state and kinetic properties of sodium channels experimentally, we here report a computer model of zebrafish muscle incorporating the sodium and potassium channels, to determine whether the properties of these ion channels as described are sufficient to explain once-only firing. The rationale of our approach is first to model the voltage-clamp currents as previously described and then to systematically alter the measured parameters until once-only firing is lost, i.e. repetitive firing is obtained. This approach therefore effectively predicts the properties of these ion currents that determine once-only or repetitive firing.

Materials and methods

We used the NEURON simulation programme (version 5.2; Hines, 1993; http://neuron.duke.edu) recompiled with additional mechanisms describing the potassium and sodium currents and running on a personal computer (IBM 300PL) under Linux (Fedora core 3; Kernel version 2.4) and Windows XP. The sodium and potassium currents were described using NMODL (neuron model description language; Hines and Carnevale, 2000). Both currents were derived from:

$$I = G\,m^3\,h(v - e)\,, \tag{1}$$

where I is the ionic current, G is the maximum current density, v is the membrane potential and e is the equilibrium potential of the ionic species. The variables m and h are solved, respectively, from:

$$m' = (m_\infty - m)/m_\tau(v) \tag{2}$$

$$h' = (h_\infty - h)/h_\tau(v)\,, \tag{3}$$

where m_∞ is the steady-state value of m (a variable representing the concentration of activation particles in the original Hodgkin Huxley formulation), m_τ is the steady-state value of the time constant of changes in m, h_∞ is the steady-state value of h (a variable representing the concentration of inactivation particles in the original Hodgkin Huxley formulation), and h_τ is the steady-state value of the time constant of changes in h. The values of each of the variables for m and h were determined from the steady-state variables according to the expressions:

$$m_\infty = 1/\{1 + \exp[(v - V_{50,act})/s_a]\} \tag{4}$$

$$h_\infty = 1/\{1 + \exp[(v - V_{50,inact})/s_i]\}\,, \tag{5}$$

where $V_{50,act}$, $V_{50,inact}$, s_a and s_i are the values for V_{50} (voltage of half activation) and slope of activation/inactivation, respectively, taken from Buckingham and Ali (2004). The values for m_τ and h_τ were taken as the time constants of activation or inactivation, respectively. Differential equations were solved within NEURON using the Crank–Nicholson method, details of which are available in the online NEURON documentation (http://www.neuron.yale.edu/neuron/papers/nc97/nc3p3.htm#3.3).

The cell was modelled with a single segment of diameter of 12 μm, length of 70 μm (based on measurements of muscle fibres *in situ*; D.W.A. and S.O.B., personal observations), specific membrane resistance of 1 kΩ cm^{-2} and axial resistance of 35.4 Ωcm. The model exploited the built-in feature of NEURON in which the 'd_lambda' value (the fraction of the length constant at 100 Hz) of 0.1 was used to set the number of compartments. Because this value produced a length constant considerably greater than the length of the segment, the simulations contained only one compartment. A non-specific passive conductance was inserted and set to 0.001 S cm^{-2}. The reversal potentials for sodium and potassium ions were set to +50 mV and –77 mV, respectively, and the reversal potential for the passive current was set to –70 mV, unless otherwise specified. To mimic a cell being recorded with a patch pipette, current was injected and current or voltage recorded at the same point, in the middle of the cell's length. Parameters were changed as described in the Results

Table 1. *Steady-state parameters used in simulations, as taken from Buckingham and Ali (2004), except where altered as stated in the text*

Parameter	Value
Sodium current	
Maximum conductance	7 S cm^{-2}
V_{50} of activation	7.3 mV
Slope of activation	8.4
V_{50} of inactivation	–74.5 mV
Slope of inactivation	–6
Potassium current	
Maximum conductance	0.21 S cm^{-2}
V_{50} of activation	–1.03 mV
Slope of activation	10.82
V_{50} of inactivation	–30.4 mV
Slope of inactivation	–4.4

The values for activation slope are for m^3 and n^3 for sodium and potassium, respectively.

Table 2. *Look-up table of the time constants of activation and inactivation for the sodium current used by the simulations, except where otherwise stated in the text*

Membrane potential (mV)	Time constant of activation (ms)	Time constant of inactivation (ms)
–150	0.001	0.2
–100	0.001	1.2
–75	0.01	4.2
–50	0.3	0.3
–30	0.08	0.2
0	0.08	0.08
10	0.07	0.07
20	0.06	0.06

Table 3. *Look-up table of the time constant of inactivation for the potassium current used by the simulations, except where otherwise stated in the text*

Membrane potential (mV)	Time constant of inactivation (ms)
–150	33
–100	33
–75	33
–50	32
–30	29
0	22
10	7
20	5

section. The values for the steady-state properties were taken from Buckingham and Ali (2004), and the values are shown in Table 1. The time constants for inactivation were taken from the original data over the range –35 mV to +60 mV, and the data for ranges more negative than –70 mV were taken as the rate of recovery from inactivation, assuming inactivation and recovery from inactivation to be the same simple transition passing in opposite directions. The rate of activation was estimated from the data in Buckingham and Ali (2004) and adjusted to produce current traces in response to voltage-clamp steps that resembled the actual recordings. These time constants were supplied to the programme as look-up tables (Tables 2, 3) for interpolation. To simplify the model, and where experimental data are lacking or incomplete, we made some assumptions about the time constants of activation and inactivation of the currents. We assumed that inactivation and recovery from inactivation can be represented by a simple set of transitions, the time constants for which in both directions have an identical voltage dependency. The time constants of activation for both sodium and potassium are difficult to measure with any accuracy and therefore have not been reported. For potassium, a simple voltage-independent value of 1 ms was assumed, whereas for sodium the values shown in Table 2 were estimated from fig. 4 of Buckingham and Ali (2004) and adjusted to produce currents that resembled those recorded *in situ*. Values for the time constant of inactivation for potassium were derived from Buckingham and Ali (2004) and are shown in Table 3. Pilot simulations revealed a sharp dependency of the time course of the sodium current upon the inactivation time constant, especially at membrane potentials at which sodium currents begin to appear (–40 to –30 mV). Since the rate of inactivation and the rate of recovery from inactivation at these potentials are unknown, we adjusted the values for this transition at these membrane potentials until currents with realistic time courses were achieved. The values that were obtained in this way (0.3 ms at –50 mV and 0.2 ms at –30 mV) are in reasonable agreement with the experimental data.

Reliable values for the V_{50} and slope of activation and inactivation for the sodium and potassium currents are available (Buckingham and Ali, 2004), so we considered these to be fixed parameters, except where these parameters were under study. The maximum conductances of the sodium and potassium currents were adjusted until their peak currents matched those in real voltage-clamp experiments; maximum conductance values of 7 and 0.21 S cm^{-2}, respectively, were found to result in currents of the appropriate amplitudes (Fig. 1). No other parameters had to be adjusted to produce currents that resembled those observed in similar experiments *in situ*.

Results

Modelling of in situ *voltage-clamp currents*

Currents in response to a series of depolarizations from –70 to +60 mV closely resembled those recorded *in situ* (Fig. 1), although the $V_{50,act}$ was shifted by ~10 mV in the depolarizing direction and the Boltzmann slope of activation also reduced. We attempted to adjust the time constants of activation to correct this but found that, although compensatory shifts in V_{50} could be achieved by speeding activation and slowing inactivation, the *I–V* curves and the time courses of the currents

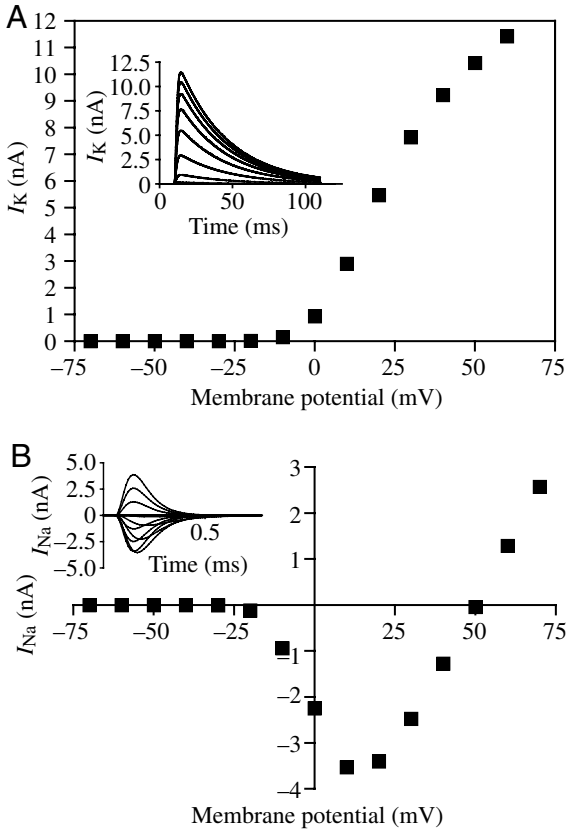

Fig. 1. Potassium currents (I_K) and sodium currents (I_{Na}) generated in a voltage-clamp simulation. (A) The simulated potassium currents are those obtained during 100 ms depolarizations from a holding potential of –90 mV to a range of potentials from –70 to +60 mV in 10 mV steps. (B) The simulated sodium currents were those obtained in response to a 1 ms depolarization to a range of potentials from –70 to + 70 mV in 10 mV steps.

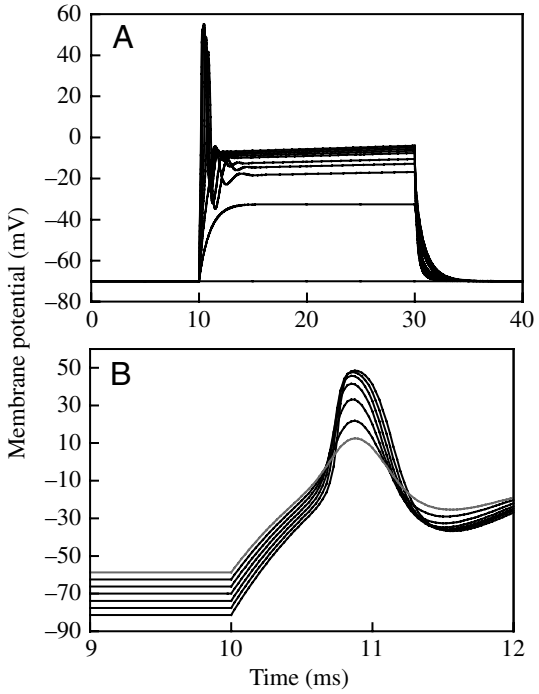

Fig. 2. Simulated current-clamp experiments in which the model muscle fibre was depolarized from resting potentials of around –70 mV. (A) The depolarizing current was increased from 1 nA to 10 nA in 1 nA steps. In no trace is repetitive discharging observed. (B) Simulated spikes elicited by a 3 nA depolarization immediately following a 10 ms prehyperpolarizing pulse ranging from 0 (red trace) to 0.6 nA (in 0.1 nA steps; black traces) are progressively reduced in amplitude.

differed from those recorded *in vivo*. We therefore conclude that the difference between the model and *in situ* values for $V_{50,act}$ and the Boltzmann slope is due to inaccuracies in assuming that the peak inward current is proportional to the maximum conductance at any membrane potential. These inaccuracies arise because the similar values for the time constants of activation and inactivation introduce errors in estimating Hodgkin Huxley parameters (*m* and *h*) from peak currents. Imperfect space clamp in whole-cell patch-clamp recordings of muscles may be a further source of error. Improper voltage control will lead to an underestimation of current amplitudes and increases in the time constants of activation. To confirm that adequate voltage clamp conditions were met, we ensured that series resistances were less than 5 MΩ before compensation, that Na^+ currents reached their peak within 500 μs and that the Na^+ currents reversed within 5–10 mV of their theoretical reversal potential (Sontheimer et al., 1992; Buckingham and Ali, 2004). In addition, any cells showing uncontrolled regenerative inward currents were omitted from our study (Eliasof et al., 1987). As a result, we favour the interpretation that the muscle cells in our study were space clamped well enough to reduce this source of error to acceptable levels. However, since our simulations explore the effects of varying steady-state and kinetic properties as independent variables, we proceeded with the values described above.

Firing properties of simulated cells under current clamp

We ran simulations of current-clamp experiments to determine the resultant firing properties of the model. Currents less than 2 nA did not evoke spikes, but currents of ⩾3 nA evoked one, and only one, spike (Fig. 2A). More than one spike was never observed at currents up to 10 nA, at which level of depolarization the first spike began to appear distorted. As was reported for spikes recorded *in situ* (Buckingham and Ali, 2004), the action potentials recorded in our simulations were graded, being of lower amplitude when evoked from more depolarized potentials (Fig. 2B).

In current-clamp experiments (Buckingham and Ali, 2004), zebrafish muscle can follow a series of depolarizing pulses with action potentials, provided the pulses are separated by a hyperpolarization. The same phenomenon is supported by our modelled cell (Fig. 3A). Indeed, the model also accurately mimicked the graded recovery of the action potential as the inter-pulse interval is increased (Fig. 3B), as well as the

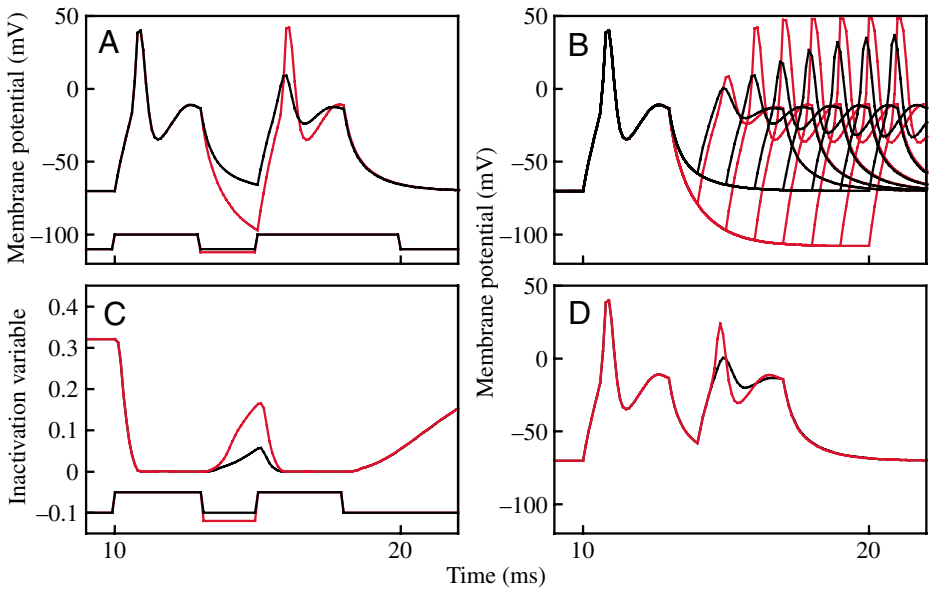

Fig. 3. Simulated muscle fibres are able to support spikes in response to rapid depolarizations (A; black trace), which is enhanced when successive stimuli are separated by a hyperpolarizing interval (A; red trace). (B) The rate of recovery of the graded action potentials in response to the second depolarization is faster when the cell is hyperpolarized by injecting 0.7 nA of current during the interstimulus interval (red traces) than when no current is injected (black traces). (C) A recording of the value of the sodium inactivation variable, *h*, between two depolarizing stimuli separated by an interval of 1 ms shows that *h* recovers more effectively when 2 nA of hyperpolarizing current is injected during the interstimulus interval (red trace) compared with 'control' (black trace). (D) If, however, the value of *h* between the paired stimuli against an interpulse potential of –70 mV is adjusted to the value that is recorded at the same time but against an interpulse potential of –90 mV (red trace), the recovery of the second action potential matches that obtained against a resting potential of –90 mV.

dependence of the rate of spike recovery upon the inter-stimulus holding potential (Fig. 3B). In our previous paper, we surmised that once-only firing is a result of a requirement for inter-stimulus hyperpolarization, whose effect is to remove inactivation of the sodium current. An analysis of the value of the inactivating state variable of the sodium current showed that hyperpolarization to around –90 mV between two successive pulses does indeed significantly increase the value compared with hyperpolarization to –70 mV (Fig. 3C). To determine whether this difference in the inactivation state particle is responsible for differences in the rate of spike recovery, we performed a dual pulse simulation similar to that in Fig. 3A and halted it 0.025 ms before the second stimulation, at which point we set the value of the inactivation particle to 0.1205, the value obtained at the same time when the simulation is run with an interpulse 0.7 nA hyperpolarization. The simulation was then allowed to continue. The resulting second spike showed partial recovery to full amplitude (Fig. 3D). This provides evidence that, in our simulation at least, the difference between spike recovery at these two potentials is attributable to the inactivation state of the sodium current.

Determination of the parameters that affect once-only or repetitive firing

Co-varying V_{50} *of activation and inactivation and time constant of inactivation of the sodium current*

To determine the parameters of the sodium current that determine whether a sustained depolarization will result in a single spike or a train of spikes, we systematically varied a number of parameters in the model of the sodium current. In the first set of simulations, we varied the $V_{50,act}$ values for the sodium current from –50 mV to +5 mV in 5 mV steps, and for each value of $V_{50,act}$ we varied the $V_{50,inact}$ from –90 mV to +5 mV in 5 mV steps. The number of action potentials during a 50 ms depolarization from a resting potential of –70 mV was counted. The runs were then sorted according to whether they elicited no action potentials, only one action potential or more than one action potential. The data were then plotted as a two-dimensional matrix with $V_{50,act}$ and $V_{50,inact}$ as the independent variables (Fig. 4). Because the action potentials were graded, we chose to select the criterion for an action potential as any spike that crosses +20 mV. Increasing the depolarizing current shifts the diagonal border between once-only firing (red region, Fig. 4A) and no response (black region, Fig. 4A) but does not significantly shift the areas in which repetitive firing occurs (green region, Fig. 4A, reading from left to right). This more amply illustrates our previous finding that increasing the level of depolarization does not lead to repetitive firing. When the time constant of inactivation is doubled (slowing the rate of inactivation), the area of parameter space over which repetitive firing is obtained is increased (Fig. 4B). However, increasing the amplitude of the depolarizing currents still did not greatly increase the area of repetitive firing.

Co-varying current density and rate of inactivation of the sodium current

It seemed plausible that the current densities of both sodium and potassium currents might affect the firing pattern. We therefore mapped the firing pattern of the model against the conductance density for both currents (Fig. 5). Altering either conductance density did not induce repetitive firing except at very high sodium current densities (more than a factor of 10; Fig. 5A). It has been suggested that slowing the rate of

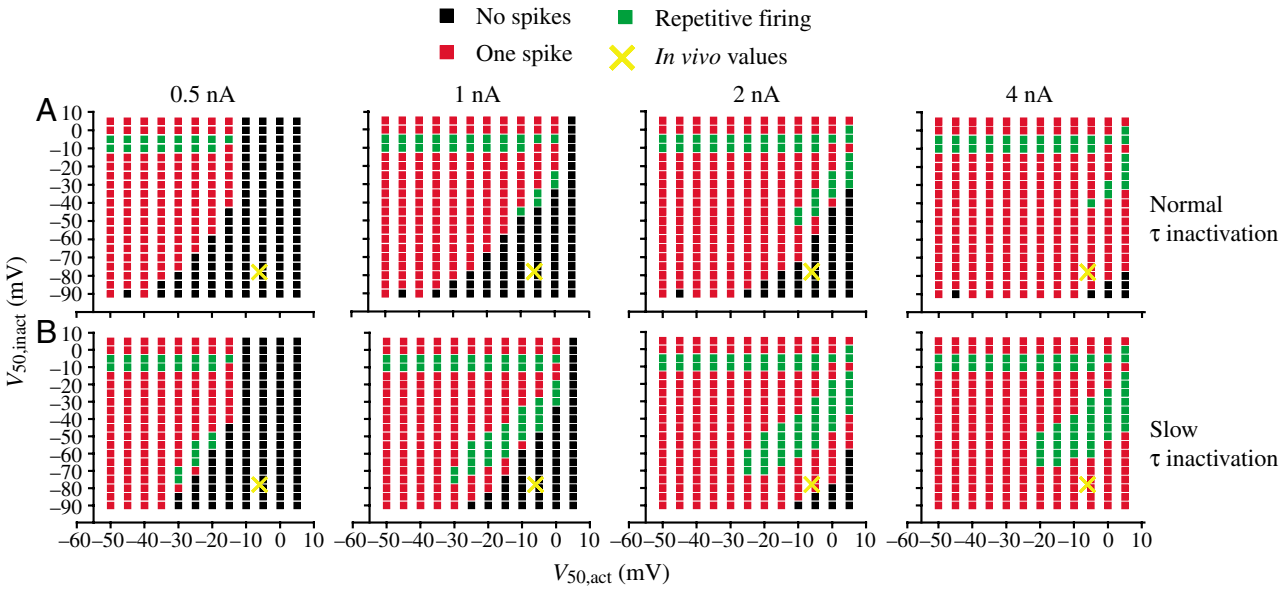

Fig. 4. Mapping of firing properties of the simulated zebrafish muscle onto the V_{50}s of activation and inactivation of the sodium current. In each graph, the $V_{50,act}$ is plotted against the $V_{50,inact}$. This was repeated for stimuli of 0.5, 1, 2 and 4 nA (left to right in each row). The values obtained from *in situ* recordings (Buckingham and Ali, 2004) are indicated with an ×. (A) When the time constant of inactivation is set to those values recorded experimentally (along with those estimated for missing values of membrane potential; see Results), increasing the amplitude of the depolarizing stimulus increases the parameter space over which single spiking is observed but does not greatly increase the area over which repetitive firing is observed between the 1 nA and 4 nA stimuli. (B) If the values of the time constant of inactivation at every membrane potential are doubled (representing a slowing of inactivation), the area of parameter space over which repetitive firing is obtained increases and approaches the parameter set observed *in situ*, but it is not affected by increasing stimulus amplitude (left to right). Repetitive firing was defined as the occurrence of more than one spike. Black areas, no spikes obtained; red areas, once-only firing; green areas, repetitive firing.

inactivation of voltage-gated sodium currents can result in changes in firing properties (Cantrell and Catterall, 2001). A marked change in firing pattern was observed in our model by slowing the rate of inactivation of the sodium channel by multiplying it by 2 (Fig. 5B) or 4 (Fig. 5C).

Slope of activation and inactivation of the sodium current

A shift from once-only firing to repetitive firing in spider mechanosensory cells required a change in the slope of activation of a sodium current (Torkkeli and French, 2002). We simultaneously varied the slope of both activation and inactivation for the sodium current from ±3 to ±9.8 in 0.2 steps. Although two spikes could be elicited for some values, repetitive firing was never obtained over these ranges of values.

Altering potassium current parameters

Simultaneously varying the $V_{50,act}$ and $V_{50,inact}$ of the potassium current between –40 mV and +10 mV and between –60 mV and +10 mV, respectively, did not produce repetitive firing. Increasing the time constant of activation of the potassium current from 1 to 2, 4, 8 or 16 ms also failed to produce either repetitive firing or dampened oscillations. Similarly, doubling the time constant of inactivation failed to produce repetitive firing as the $V_{50,act}$ and $V_{50,inact}$ were varied over this same range.

Discussion

Here, we model the ion currents we reported in a previous recent publication to determine whether such a description of those currents is sufficient to explain the phenomenon of once-only firing observed in zebrafish larval skeletal muscle. The model demonstrates that without having to alter the values of $V_{50,act}$ and $V_{50,inact}$ or the slopes of activation or inactivation or the levels of current expression, these currents do indeed generate once-only firing, once the time constants for inactivation and activation are adjusted to produce currents that resemble those observed in voltage-clamp experiments. This argues that it is not necessary to invoke any extra currents, such as voltage-gated chloride currents, although it does not show that such currents do not contribute to the phenomenon *in situ*.

Our model differs from *in vivo* patch-clamp recordings in that it does not take into account possible errors arising from inadequate space clamp. Simulated current injections produced membrane potential deflections that did not differ along the length of the fibre. The same was seen when the model cell was divided into 50 compartments (data not shown). Thus, the model had good space clamp. Whole-cell patch-clamp recordings from muscle, however, suffer from imperfect space clamp, as well as errors arising from the series resistance of the recording pipette. In our previous study, we confirmed adequate space clamping of the muscle fibres by only using cells that did not show any uncontrolled

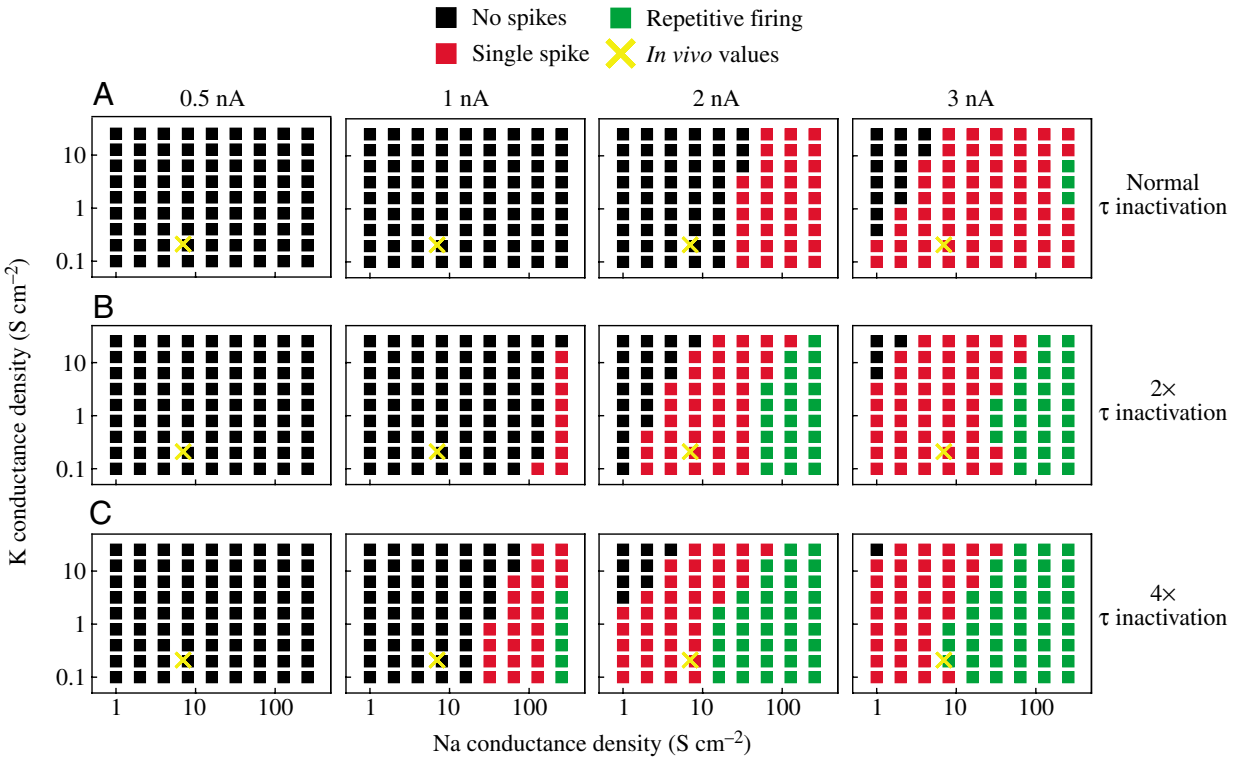

Fig. 5. Mapping of firing properties of the simulated zebrafish muscle cell onto the maximum conductance densities of the potassium and sodium currents at different rates of inactivation. The values obtained from *in situ* recordings (Buckingham and Ali, 2004) are indicated with an ×. (A) At the control rate of inactivation, repetitive firing was not observed, even when the level of sodium current is multiplied more than 10-fold, and is little affected by the level of the potassium current. (B) When the values of the time constant of inactivation at all membrane potentials are multiplied by 2, the range of values over which repetitive firing is obtained is greatly increased. (C) Multiplying the values of the time constant by 4 increases the area still further. Black areas, no spikes obtained; red areas, once-only firing; green areas, repetitive firing.

regenerative inward currents and in which the Na^+ currents occurred within several hundred microseconds from the onset of the voltage steps. Lastly, we ensured that Na^+ currents reversed within 5–10 mV of the theoretical reversal potential. It is possible that a lack of adequate space clamping could negate our ability to record more than a single spike, but we were confident that we had adequate voltage control of our cells and that the single spike phenomenon we recorded is also seen *in vivo*. Buckingham and Ali (2004) estimate that series resistance in their recordings could amount to 3–5 mV and membrane-charging time constants to the order of 12–15 μs after 85% series resistance compensation using the amplifier's circuitry. These differences in space clamp are not taken into account by our model.

The values for the inactivation rate of the sodium current had to be adjusted to produce sodium currents under voltage clamp with properties resembling those of *in situ* currents. This is probably attributable to errors in estimating these values from patch-clamp recordings, arising from the fact that it is difficult to measure rates of activation from rapidly inactivating currents where activation is incomplete before significant inactivation occurs. Although this would be a potentially serious source of error in the model if *in situ* data were used naively, it is assumed that at least some of this error is compensated for by the adjustments to the values of time constant performed to produce realistic currents.

When $V_{50,act}$ and $V_{50,inact}$ are mapped (Fig. 4) against each

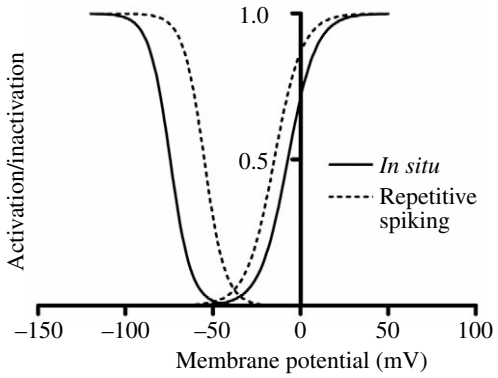

Fig. 6. The steady-state activation and inactivation properties of the sodium currents required to produce repetitive firing in the model (dotted lines) are compared with those reported *in situ* (solid lines). The V_{50}s of activation and inactivation required were taken as the coordinates in Fig. 4 of the point that represents the minimum distance from the values obtained *in situ*. Note that for repetitive firing to occur, there must be a simultaneous right shift in inactivation and a left shift in activation.

other in terms of the firing properties that they produce, it can be seen that the values obtained in voltage-clamp experiments on zebrafish muscle *in situ* lie in a position away from where repetitive firing is obtained. This suggests that currents that can be described in this way are unlikely to mediate repetitive firing unless significant changes to their properties are made. Where the data are mapped as in Fig. 4, the minimum change in $V_{50,act}$ and $V_{50,inact}$ required to bring about repetitive firing is represented by the shortest line from the *in situ* values to the borderline of the area in which repetitive firing is obtained. The coordinates of the end of this line represent the steady-state values at which repetitive firing is obtained, and in the model this represents a convergence of the steady-state curves to bring about an increased overlap (Fig. 6). A number of studies have shown that some steady-state parameters and maximum current density of voltage-gated sodium channels can be modulated by intracellular enzymes such as tyrosine kinases and phosphatases (Alroy et al., 1999; Hilborn et al., 1998; Ratcliffe et al., 2000) or by second messengers such as G-protein subunits (Ma et al., 1994, 1997). However, the model reported here suggests that the inactivation rate of the sodium current must be at least quadrupled if the firing properties of the cell are to change from once-only firing to repetitive discharges. Alternatively, the model suggests that such a change of firing properties could be effected by a simultaneous rightward shift in inactivation and a leftward shift in activation. These steady-state changes differ from those of Torkkeli and French (2002), except that both mechanisms are due primarily to the amount of sodium channel inactivation. However, a number of other groups have found a variety of mechanisms for once-only firing. For instance, a large amount of sodium inactivation coupled with an insufficient sodium conductance is thought to be responsible for the single-spike firing in retinal amacrine cells of the tiger salamander (Eliasof et al., 1987). Neurons of the medial nucleus trapezoid body relay synaptic information and follow presynaptic action potentials at frequencies up to 600 Hz (Wu and Kelly, 1993). These neurons fire single spikes in response to long depolarizing steps and can be induced to fire multiple action potentials when potassium channels are blocked by dendrotoxin (Brew and Forsythe, 1995). Single-spike firing may also be developmentally regulated when the influence of an $I_{K(Ca)}$ is strong and results in once-only firing at early postnatal stages (Rothe et al., 1999). We conclude from our findings that the changes necessary to affect the firing properties of the cells are greater than are likely to be observed in real cells and that the sodium channels of zebrafish muscle are optimized to prevent repetitive discharge and ensure once-only firing even at high levels of excitation.

Our parameter mapping approach has shown that, in our computer model, the parameter that most affects whether once-only or repetitive firing is obtained is the time constant of inactivation of the sodium current. Although the most common use of the somatic tail muscle will be in swimming, it is likely that it is also used in postural behaviours, not all of which require rapid pulsatile contractions. Indeed, our model suggests that, with the steady-state and kinetic properties reported using voltage clamp, the muscles would not be able to maintain a sustained contraction, making tonic posture control difficult. It is tempting to speculate that a switch from phasic to tonic control of the muscle might be made possible by modulation of the sodium current, which effects an increase in the time constant of inactivation together, possibly, with an effective increase in the sodium current density or the $V_{50,act}$ and $V_{50,inact}$. As argued above, there is evidence that such mechanisms exist, although it is unclear whether alterations in kinetics or steady-state properties through intracellular modulation of voltage-gated ion channels would be fast enough to allow such switching. Further, adaptations for once-only firing are also evident in two elements of the afferent pathway: motor neurones to these muscles respond to a sustained depolarization with a short burst consisting of only a few spikes (Buss et al., 2003), and the Mauthner neuron, which is presynaptic to the primary afferents, also exhibits once-only firing (Charpier et al., 1995; Hatta and Korn, 1998; Korn et al., 1990). It is of interest that three consecutive elements in this motor pathway are primed to ensure high-pass filtering.

We have shown in a previous paper that the maximum rate of full spiking in response to pulsatile stimulation is dependent upon the inter-stimulus membrane potential (Buckingham and Ali, 2004), and we suggested that this might reflect the dependence of the recovery from inactivation of the sodium channel. This model confirms this, as artificially resetting the state of the sodium inactivation particle to a value obtained at resting potentials of –90 mV restores the amplitude of the following spike. As yet, we know of no way of imitating this experimentally.

Our findings show no role for the potassium current in ensuring once-only firing, as no perturbation of the potassium current succeeded in bringing about repetitive firing.

References

Adrian, R. H. and Bryant, S. H. (1974). On the repetitive discharge in myotonic muscle fibres. *J. Physiol.* **240**, 505-515.

Alroy, G., Su, H. and Yaari, Y. (1999). Protein kinase C mediates muscarinic block of intrinsic bursting in rat hippocampal neurons. *J. Physiol.* **518**, 71-79.

Bretag, A. H. (1987). Muscle chloride channels. *Physiol. Rev.* **67**, 618-724.

Brew, H. M. and Forsythe, I. D. (1995). Two voltage-dependent K^+ conductances with complementary functions in postsynaptic integration at a central auditory synapse. *J. Neurosci.* **15**, 8011-8022.

Bryant, S. H. (1962). Muscle membrane of normal and myotonic goats in normal and low external chloride. *Fed. Proc.* **21**, 312.

Buckingham, S. D. and Ali, D. W. (2004). Sodium and potassium currents of larval zebrafish muscle fibres. *J. Exp. Biol.* **207**, 841-852.

Buss, R. R. and Drapeau, P. (2000). Physiological properties of zebrafish embryonic red and white muscle fibres during early development. *J. Neurophysiol.* **84**, 1545-1557.

Buss, R. R. and Drapeau, P. (2002). Activation of embryonic red and white muscle fibers during fictive swimming in the developing zebrafish. *J. Neurophysiol.* **87**, 1244-1251.

Buss, R. R., Bourque, C. W. and Drapeau, P. (2003). Membrane properties related to the firing behavior of zebrafish motoneurons. *J. Neurophysiol.* **89**, 657-664.

Cantrell, A. R. and Catterall, W. A. (2001). Neuromodulation of Na^+ channels: an unexpected form of cellular plasticity. *Nat. Rev. Neurosci.* **2**, 397-407.

Charpier, S., Behrends, J. C., Triller, A., Faber, D. S. and Korn, H. (1995). "Latent" inhibitory connections become functional during activity-dependent plasticity. *Proc. Natl. Acad. Sci. USA* **92**, 117-120.

Drapeau, P., Ali, D. W., Buss, R. R. and Saint-Amant, L. (1999). *In vivo* recording from identifiable neurons of the locomotor network in the developing zebrafish. *J. Neurosci. Methods* **88**, 1-13.

Eliasof, S., Barnes, S. and Werblin, F. (1987). The interaction of ionic currents mediating single spike activity in retinal amacrine cells of the tiger salamander. *J. Neurosci.* **7**, 3512-3524.

Greer-Walker, M. and Pull, G. A. (1975). A survey of red and white muscle in marine fish. *J. Fish Biol*. **7**, 295-300.

Hatta, K. and Korn, H. (1998). Physiological properties of the Mauthner system in the adult zebrafish. *J. Comp. Neurol*. **395**, 493-509.

Hilborn, M. D., Vaillancourt, R. R. and Rane, S. G. (1998). Growth factor receptor tyrosine kinases acutely regulate neuronal sodium channels through the Src signaling pathway. *J. Neurosci*. **18**, 590-600.

Hines, M. (1993). NEURON – a simulation program for simulation of nerve equations. In *Neural Systems: Analysis and Modelling* (ed. F. Eeckman and M. A. Norwell), pp. 127-136. Boston, MA: Kluwer Academic Publishers.

Hines, M. L. and Carnevale, N. T. (2000). Expanding NEURON's repertoire of mechanisms with NMODL. *Neural Comput.* **12**, 839-851.

Korn, H., Faber, D. A. and Triller, A. (1990). Convergence of morphological, physiological, and immunocytochemical techniques for the study of single Mauthner cells. In *Handbook of Chemical Neuroanatomy*, vol. 8 (ed. A. Bjorklund, T. Hokfelt, F. G. Wouterlood and A. N. van den Pol), pp. 403-480. New York: Elsevier Science Publishers.

Ma, J. Y., Li, M., Catterall, W. A. and Scheur, T. (1994). Modulation of brain Na^+ channels by a G-protein-coupled pathway. *Proc. Natl. Acad. Sci. USA* **91**, 12351-12355.

Ma, J. Y., Catterall, W. A. and Scheur, T. (1997). Persistent sodium current through brain sodium channels induced by G protein βγ subunits. *Neuron* **19**, 443-452.

Ratcliffe, C. F., Qu, Y., McCormick, K. A., Tibbs, V. C., Dixon, J. E., Scheur, T. and Catterall, W. A. (2000). A sodium channel signaling complex: modulation by associated receptor protein tyrosine phosphatase β. *Nat. Neurosci*. **3**, 437-444.

Rothe, T., Bahring, R., Carroll, P. and Grantyn, R. (1999). Repetitive firing deficits and reduced sodium current density in retinal ganglion cells developing in the absence of BDNF. *J. Neurobiol*. **40**, 407-419.

Seyfarth, E.-A. and French, A. S. (1994). Intracellular characterization of identified sensory cells in a new spider mechanoreceptor preparation. *J. Neurophysiol.* **71**, 1422-1427.

Sontheimer, H., Black, J. A., Ransom, B. R. and Waxman, S. G. (1992). Ion channels in spinal cord astrocytes in vitro I. Transient expression of high levels of Na^+ and K^+ channels. *J. Neurophysiol*. **68**, 985-1000.

Torkkeli, P. H. and French, A. S. (2002). Simulation of different firing patterns in paired spider mechanoreceptor neurons: the role of Na^+ channel inactivation. *J. Neurophysiol*. **87**, 1363-1368.

Tsutsui, H. and Oka, Y. (2002). Slow removal of Na^+ channel inactivation underlies the temporal filtering property in the teleost thalamic neurons. *J. Physiol*. **539**, 743-753.

Tsutsui, H., Yamomoto, N., Ito, H. and Oka, Y. (2001). Encoding of different aspects of afferent activities by two types of cells in the corpus glomerulosum of a teleost brain. *J. Neurophysiol*. **85**, 1167-1177.

Van Raamsdonk, W., Moss, W., Tekronnie, G., Pool, C. W. and Mijzen, P. (1979). Differentiation of the musculature of the teleost *Brachydanio rerio*. II. Effects if immobilization on the shape and structure of somites. *Acta. Morphol. Neerl-Scand*. **17**, 259-274.

Westerfield, M. (2000). *The Zebrafish Book: A Guide For The Laboratory Use Of Zebrafish* (*Danio rerio*). 4th edn. Eugene, OR: University of Oregon Press.

Westerfield, M., McMurray, J. V. and Eisen, J. S. (1986). Identified motoneurons and their innervation of axial muscles in the zebrafish. *J. Neurosci*. **6**, 2267-2277.

Wu, S. H. and Kelly, J. B. (1993). Response of neurons in the lateral superior olive and medial nucleus of the trapezoid body to repetitive stimulation: intracellular and extracellular recordings from mouse brain slice. *Hearing Res*. **68**, 189-201.